European Polymer Journal 180 (2022) 111607

Contents lists available at ScienceDirect

European Polymer Journal

journal homepage: www.elsevier.com/locate/europolj

Real-Time ^{1}H and ^{31}P NMR spectroscopy of the copolymerization of cyclic phosphoesters and trimethylene carbonate reveals transesterification from gradient to random copolymers

Timo Rheinberger [a], Marc Ankone [b], Dirk Grijpma [b], Frederik R. Wurm [a,*]

[a] Sustainable Polymer Chemistry (SPC), Department for Molecules and Materials, MESA+ Institute for Nanotechnology, Faculty of Science and Technology, University of Twente, P.O. Box 217, 7500 AE Enschede, Netherlands
[b] Department of Biomaterials Science and Technology, Faculty of Science and Technology, University of Twente, Enschede, the Netherlands

ARTICLE INFO

Keywords:
Polyphosphoester
Trimethylene carbonate
Microstructure
Polycarbonate
Transesterification

ABSTRACT

Copolymerization is the general approach to combine properties of different polymers in a single material. We prepared the first trimethylene carbonate (TMC) phosphoester (PE) copolymers by statistical copolymerization using either stannous octanoate or 1,8-diazabicyclo[5.4.0]undec-7-ene (DBU) as the respective catalyst. Variation of comonomer feed, reaction temperature and solvent, resulted in a library of copolymers with molar masses of up to 83,000 g/mol and moderate molar mass dispersities (<1.8). The monomer consumptions during the copolymerizations were followed by real-time ^{1}H and ^{31}P NMR spectroscopy in solution and in the bulk. As ring-opening copolymerization of cyclic esters often leads to gradient copolymers, also TMC and PE co-polymerizations resulted in gradient copolymers, i.e. P(TMC-*grad*-PE)s, with different gradient strength depending on the copolymerization conditions. If a suitable transesterification catalyst like stannous octanoate was used, randomization of the gradient copolymer occurred. The ^{31}P NMR shift of incorporated phosphoester units was used as a probe to monitor the randomization of the gradient copolymers in real-time by ^{31}P NMR spectroscopy. The P-comonomer acts as an ideal NMR probe for *in situ* monitoring the changes of the copolymers' microstructure during the transesterification by following the evolution of diads and triads. This paper focusses on the randomization procedure and gives detailed information about the copolymer structure and the kinetics of the copolymerization. The data give the possibility to understand randomization processes on a molecular scale and to fine-tune properties of polycarbonate-polyphosphoester copolymers in future applications.

1. Introduction

Copolymers based on cyclic esters and carbonates are used as biodegradable materials for medical applications or in packaging.[1–3] Statistical ring-opening copolymerization of cyclic ester monomers is a typical way to prepare such copolymers, however, different comonomer combinations can lead to gradient or random copolymers.[4] Further, catalyst type and reaction conditions also influence the copolymers' microstructure and the resulting macroscopic properties, such as mechanical, thermal, degradation profiles or phase separation.[5–8] The comonomer distribution is often not known or neglected and in many cases hard to detect in the final product due to signal overlap in NMR spectroscopy.

Herein, we prepared a novel type of potentially biodegradable and biocompatible copolymers based on poly(trimethylene carbonate)[9] and polyphosphoesters (PPEs)[10] and we used the chemical shift of the phosphorus-containing monomer as a sensitive probe for determining the copolymers' microstructure.[11,12].

To optimize the material properties, it is important to know the monomer distribution along the copolymer chain. Statistical copolymerization can result in block, gradient, or random copolymer microstructures, which are hard to detect spectroscopically in the final product.[13] Typically, ^{13}C NMR is used to detect diads or triads in the copolymers,[14] i. a. copolyesters.[15] For polyphosphoesters, we previously used ^{31}P NMR to determine diad sequences in copolymers.[12] Another way of determining the comonomer sequence in living or controlled polymerizations is the use of real-time NMR spectroscopy, i.e. following the monomer consumptions during the copolymerization,

* Corresponding author.
E-mail address: f.r.wurm@utwente.nl (F.R. Wurm).

https://doi.org/10.1016/j.eurpolymj.2022.111607
Received 16 August 2022; Received in revised form 21 September 2022; Accepted 22 September 2022
Available online 27 September 2022
0014-3057/© 2022 The Authors. Published by Elsevier Ltd. This is an open access article under the CC BY license (http://creativecommons.org/licenses/by/4.0/).

which has been used previously via ^{1}H,[16,17] ^{13}C,[18] or ^{31}P NMR spectroscopy in solution.[19] For polymerizations in the bulk it is not easy to follow the polymer formation *in situ* due to high viscosity preventing NMR techniques to be used and mainly off-line techniques (taking samples) are used to follow copolymerization kinetics. Bulk polymerizations have certain advantages, they do not need a solvent, which has to be removed afterwards and due to the high monomer concentration polymers with high degree of polymerization can be achieved.

The molar mass determines mechanical properties. One monomer, which is polymerized in bulk to achieve high molar mass biodegradable polymers, is trimethylene carbonate.[20,21] Poly(trimethylene carbonate) (PTMC) is used in biomedical research for different applications, e.g. for drug delivery or in tissue engineering (Maxon, Inion CPS).[22] To tune the mechanical as well as the degradation properties, PTMC was copolymerized or blended with different other biocompatible polymers like poly(ε-caprolactone) (PCL), polylactide (PLA), or polyglycolide (PGA).[9] The copolymerization is often catalyzed by stannous octanoate ($Sn(Oct)_2$), which is also well-known to catalyze transesterification reactions,[23,24] further complicating the analysis of the polymer structure during the copolymerization.

Here, we prepared poly(TMC-*co*-PE) copolymers using the P-containing monomer as a probe for combined ^{1}H/^{31}P real-time NMR kinetics but also to explore a new class of PTMC-copolymers. Different conditions resulted in a library of copolymers with various gradient structures. Further, the gradient copolymers were randomized using $Sn(Oct)_2$ and the randomization kinetics were followed by ^{31}P NMR spectroscopy.

2. Results and discussion

We performed statistical copolymerization of 2-ethyl-2-oxo-1,3,2-dioxaphospholane (EtPPn) and TMC in solution using the metal-free superbase 1,8-diazabicyclo[5.4.0]undec-7-ene (DBU) or in the bulk using the conventional $Sn(Oct)_2$ the respective catalyst and under typical reaction conditions (cf. Scheme 1). As PEtPPn is hydrophilic and water-soluble, the amount of the EtPPn comonomer in the PTMC-copolymers was adjusted between 7 and 25 % to keep the final copolymers hydrophobic that they could be suitable for applications, for which PTMC could be used, e.g. tissue engineering or implant material. The copolymerizations were conducted directly in an NMR tube and the comonomer consumption was followed by real-time ^{1}H/^{31}P NMR spectroscopy (the reaction conditions are outlined in Scheme 1).

Since the EtPPn is usually polymerized in solution (ca. 4 M in DCM, 30 °C, 16 h) with DBU as a catalyst,[25] and TMC can be polymerized under the same conditions,[26] we performed a copolymerization under these conditions. We also copolymerized TMC with EtPPn in bulk with $Sn(Oct)_2$ as it is common for PTMC. The synthesized copolymers were obtained as sticky solids, their molecular characteristics are listed in Table 1; moderate molar mass distributions ($Đ$<1.8) were obtained (cf. Fig. S2). The solution approach with DBU resulted in lower dispersities ($Đ$=1.3–1.5) compared to the bulk reaction, presumably because the initiation step can be conducted faster in solution compared to bulk conditions. For the metal-coordinated polymerization performed in the bulk, the initiation step might be slower due to inhomogeneous melting of the monomer mixture and limited heat flow. The ratio of TMC vs EtPPn in the final copolymers was quantified by ^{1}H NMR spectroscopy by comparing the integrals of the resonances of the methylene protons in position 5 of the TMC units (at 4.17 ppm) with the integrals of the resonances of the methyl protons in the side chain of the EtPPn units (at 1.10 ppm) (Fig. S1 shows the peak assignments).

When the reaction was conducted directly in an NMR tube, the consumption of both monomers can be followed *in situ* by alternating ^{1}H and ^{31}P NMR measurements. To calculate the conversion of the TMC monomer, the changes of the integrals at 4.33 ppm (in the ^{1}H NMR spectra) were followed, i.e. the methylene protons in the 4 and the 6 positions of TMC (Fig. S3). The consumption of EtPPn was calculated from the decrease of the monomer resonance at ca. 50.8 ppm and the formation of polymeric units between 34.7 and 35.3 ppm in the ^{31}P NMR spectra (Fig. S3).

During the copolymerization of TMC and EtPPn, different microstructures can be formed, which are identified by different triad structures (cf. Fig. 1b). The PPP triad, i.e. phosphonate units neighboring a central phosphonate is expected in the homopolymer or a phosphonate-rich block. With an increasing amount of TMC in the copolymer, TPP and PPT triads are expected, then TPT and finally only TTT triads. We look at the central phosphorus shift in the triads, which is influenced by the neighboring monomer unit in the copolymers. From the ^{31}P NMR measurements, we were able to quantify the formation of these different triads during the copolymerization (Fig. 1a). As EtPPn is the faster comonomer under these conditions, the initially detected signals during the copolymerization represent the PPP triads. The chemical structures of the possible triads are visualized in Fig. 1b. When the integrals of the ^{31}P NMR resonances represented each triad were plotted as a function of time, it shows that most of the PPP triads are formed in the early stages of the copolymerization, due to faster ring-opening of EtPPn at high initial concentration compared to TMC ring-opening under the respective conditions. At later stages of the reaction, the incorporation of TMC into the copolymer structure increased, as can be seen by the formation of TPP and PPT triads, followed by the formation of TPT triads. After consumption of EtPPn, the residual TMC monomer is polymerizing, leading to pure TTT triads (which are not visible in ^{31}P NMR). The signal assignment was also confirmed by 2D NMR measurements (Fig. S4) and follows the same trend as we reported for other PPE-containing copolymers.[11,12].

From the real-time NMR measurements, we calculated the respective reactivity ratios for EtPPn and TMC using different nonterminal models, as proposed by Jaacks,[27] BSL (Beckingham, Sanoja, and Lynd),[28] and Frey[29] (ideal integrated model). The kinetic data were fitted with the models and resulted in similar reactivities ratios for the solution copolymerization, i.e. r(EtPPn) = 2.4 and r(TMC) = 0.4 (we used the experimental data up to 50 % of the total monomer conversion for the calculations as recommended previously for other copolymerizations, [28] Fig. S5). Using the determined reactivity ratios from the ideal integrated model, the comonomer distribution can be visualized by plotting the polymer fraction vs conversion (Fig. 2). Further, the idealized

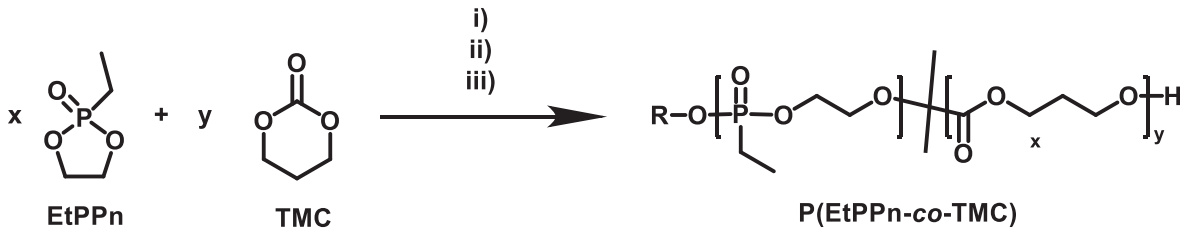

Scheme 1. Copolymerizations of 2-ethyl-2-oxo-1,3,2-dioxaphospholane (EtPPn) and trimethylene carbonate (TMC); reaction conditions: i) with 2-(methoxy)ethanol as the initiator and 1,8-diazabicyclo-[5.4.0]undec-7ene (DBU) as a catalyst in a 4 M dichloromethane solution at 25 °C, ii) with stannous octanoate ($Sn(Oct)_2$) as a catalyst in bulk at 120 °C, iii) with $Sn(Oct)_2$ as a catalyst in bulk at 130 °C (note that for ii and iii no exogenous alcohol was added as the initiator).

Table 1
Summarized properties of the synthesized P(EtPPn-*co*-TMC) copolymers.

#	catalyst	Reaction Temp.	Solution/ bulk	reaction time	Comonomer feed ratio TMC: EtPPn[a]	copolymer comp. TMC: EtPPn[a]	conversion of TMC[a]	Conversion of EtPPn[b]	M_n / g • mol^{-1}[c]	$Đ$[c]	T_g[d] / °C
1	DBU	25 °C	DCM	43 h	88: 12	83: 17	60 %	90 %	11,000	1.29	n.d.
2a[e]	DBU	25 °C	DCM	48 h	85: 15	77: 23	52 %	87 %	13,000	1.47	−25
2b[e]	DBU	25 °C	DCM	92 h	85: 15	75: 25	55 %	90 %	15,000	1.40	−30
3a[f]	Sn $(Oct)_2$	120 °C	Bulk	26 h	88: 12	n.d.	32 %	96 %	n.d.	n.d.	n.d.
3b[f]	Sn $(Oct)_2$	130 °C	Bulk	3 weeks	88: 12	90: 10	96 %	100 %	48,000	1.76	−29
4	Sn $(Oct)_2$	130 °C	Bulk	19 h	91: 9	93: 7	98 %	95 %	53,000	1.65	−25
5	Sn $(Oct)_2$	130 °C	Bulk	24 h	90: 10	88: 12	96 %	100 %	83,000	1.68	−27
6	Sn $(Oct)_2$	130 °C	Bulk	24 h	75: 25	75: 25	97 %	94 %	63,000	1.57	−29

[a] determined from ^{1}H NMR measurements,
[b] determined from ^{31}P NMR measurements,
[c] determined via GPC in DMF (0.1 M LiCl, at 50 °C) vs polystyrene standards (elugram shown in Fig. S2a),
[d] glass transition temperatures (T_g) determined from the second heating ramp in DSC measurements (Fig. S2b),
[e] **2a** is an aliquot from the reaction **2b** taken after 48 h, f) the NMR tube from the kinetic measurement **3a** was placed in an oil bath at 130 °C to induce randomization → **3b**, n.d.: as the sample 3a was used in the transesterification in a closed ampule, no polymer sample was taken.

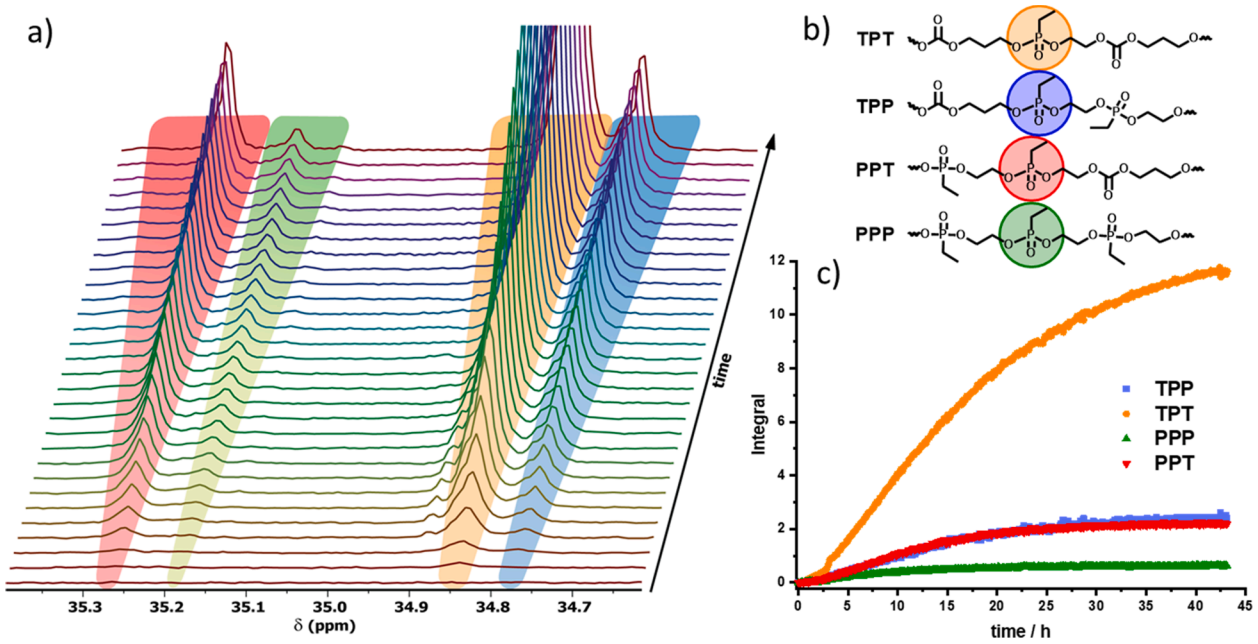

Fig. 1. Real-time ^{31}P NMR kinetics for the copolymerization of TMC and EtPPn (entry **1**, Table 1) to P(EtPPn-*co*-TMC) in solution. (a) Overlay of ^{31}P NMR of the copolymerization conducted in the NMR spectrometer; highlighted are the resonances of the different triads (interval between each measurement: 85 min). (b) Chemical structures of the four different triads, which can be distinguished from the ^{31}P NMR shift of the central P-unit. c) Integral values of the central P-unit of the different triads plotted against reaction] time.

microstructure of the resulting copolymers was calculated using a Monte Carlo simulation: we simulated the comonomer distribution for 10 polymer chains with the same theoretical degree of polymerization, as reported previously for other copolymers (Fig. 2).[30] This visualization of the copolymers' microstructure shows the formation of a gradient copolymer in the final material with a phosphorus-rich first and a TMC-rich second segment, corroborating with the identified triads from NMR spectroscopy (EtPPn monomer units are shown in yellow, TMC units are shown in blue in Fig. 2).

With the information from the reaction in solution, co-polymerizations in the bulk were performed. Since TMC is usually polymerized in the bulk with $Sn(Oct)_2$ as a catalyst, we used these conditions also for the copolymerization with EtPPn at two different temperatures, i.e. 120 °C and 130 °C (comparable conditions as for the solution polymerization did not yield any polymer materials with Sn $(Oct)_2$). The monomers, initiator and catalyst were premixed and loaded into an NMR tube, sealed, and heated so that a melt was obtained. The copolymerizations were monitored by measuring alternating ^{1}H and ^{31}P NMR spectra (cf. Experimental). As the mixture remained liquid during the reaction, the monomer consumptions could be followed on an NMR timescale and we were able to calculate reactivity ratios from the three different models also for the bulk copolymerizations (cf. Figs. S6 – S8, Table S1 for detailed information). At 120 °C, reactivity ratios of r (EtPPn) = 9.7 and r(TMC) = 0.11, i.e. a gradient profile was calculated. The reactivity ratios at 130 °C were revealed also a gradient structure, however, with r(EtPPn) = 6.1 and r(TMC) = 0.16 a softer gradient was

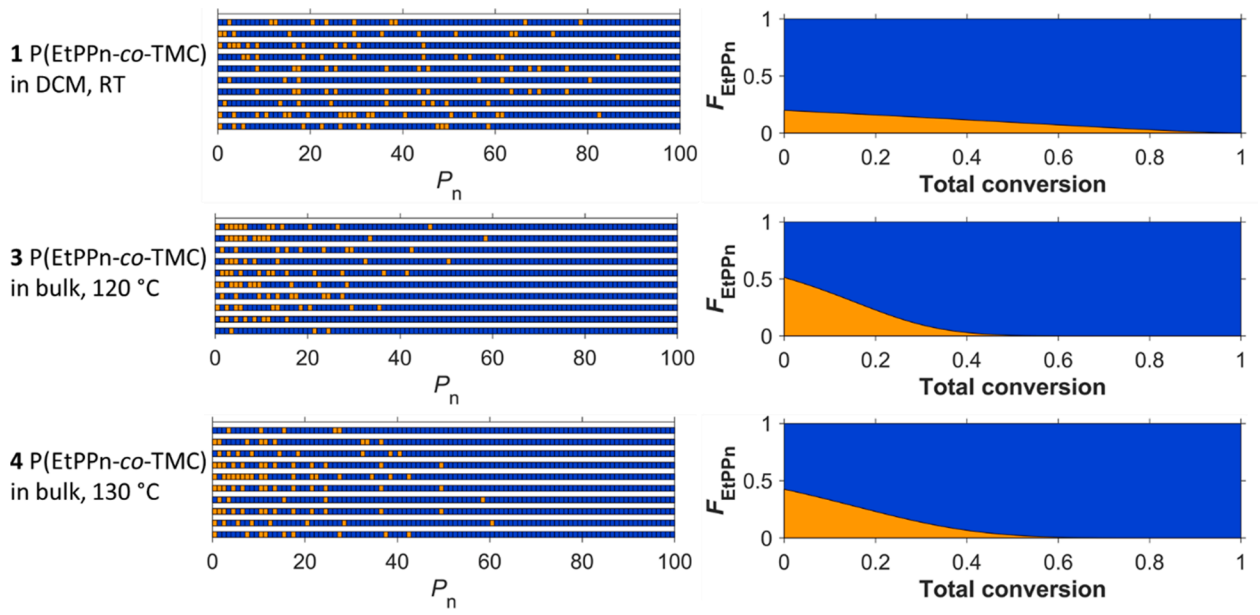

Fig. 2. Visualization of the copolymer compositions of the synthesized copolymers (without transesterification) calculated via Monte Carlo simulation using the determined reactivity ratios (*left*) and plots of the average monomer fraction composition against the total conversion (*right*) determined from the real-time NMR spectra; EtPPn shown in yellow, TMC shown in blue. (For interpretation of the references to colour in this figure legend, the reader is referred to the web version of this article.)

obtained. The comonomer distribution was calculated and visualized using the polymer fractions vs conversion and by the Monte Carlo simulations in the same way as reported for the solution polymerization (Fig. 2).[30].

As the NMR signals from the bulk copolymerization exhibited a significant peak broadening compared to the solution copolymerization, only PP and TP diads (no triads) could be differentiated from the ^{31}P NMR spectra (Fig. 3b). The reaction at 120 °C showed a steady increase

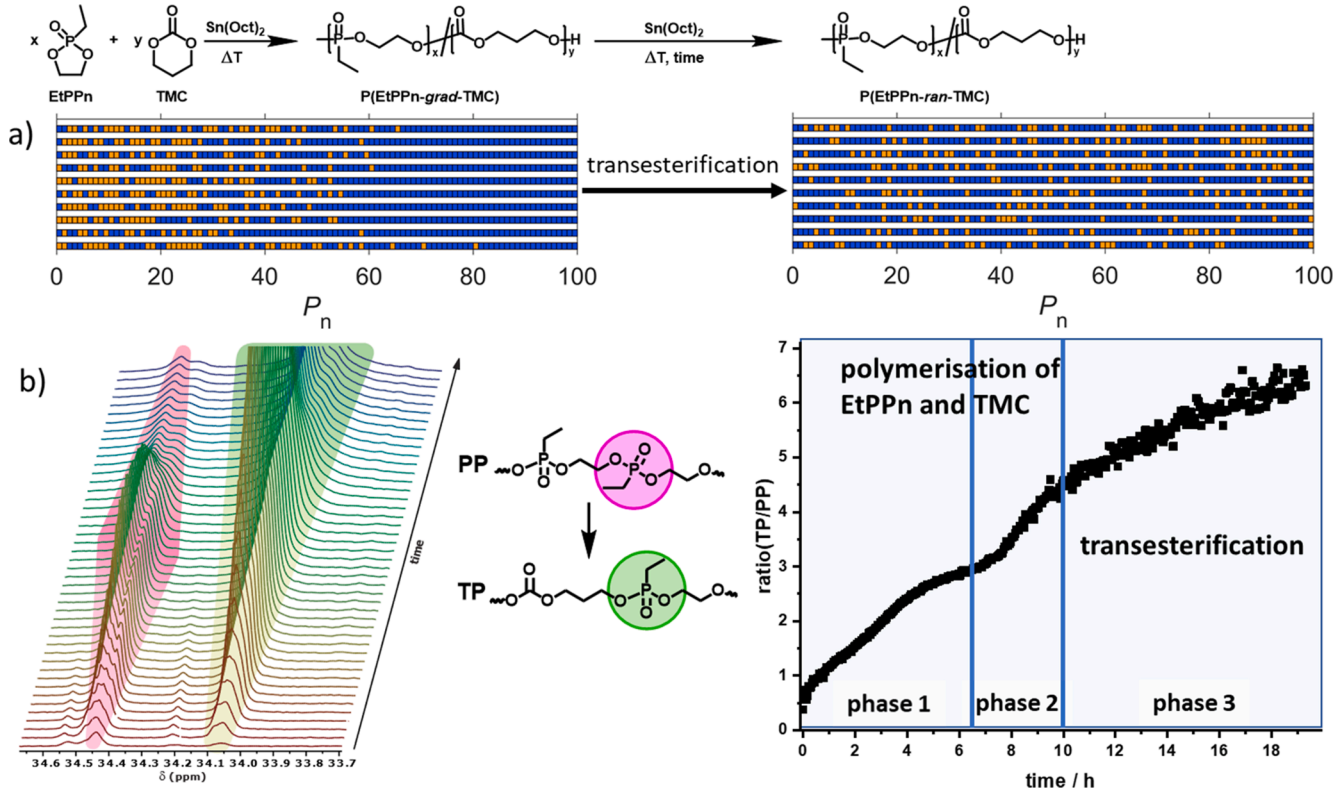

Fig. 3. Real-time ^{31}P NMR kinetics for the copolymerization of TMC and EtPPn to P(EtPPn-*co*-TMC) in the bulk with subsequent transesterification. a) Monte Carlo simulations of polymer **5**P(EtPPn-*co*-TMC): *left*: the obtained gradient structure calculated from the reactivity ratios after full monomer consumption and *right*: randomized after transesterification. b) ^{31}P NMR kinetics of polymer **4** showing the increase of the PP diads during the polymerization and the decrease during the transesterification, the ratio of these TP/PP diads is plotted against time.

for both diads (Fig. S9), for high conversions of the EtPPn monomer the PP diads signal decreased only slightly, indicating that almost no transesterification occurred during the reaction at 120 °C. After increasing the temperature, three phases during the copolymerization were observed (Fig. 3b): In the first phase, statistical copolymerization of TMC and EtPPn occurred with EtPPn being the faster-consumed comonomer. When EtPPn was consumed (i.e. after 6.5 h for the 130 °C copolymerization), the second phase adds homopolymerization of TMC to result in the gradient copolymer structures as depicted in Fig. 2. However, if the reaction is kept at 130 °C, transesterification occurred - catalyzed by $SnOct_2$. The transesterification was detected in NMR spectroscopy by a steady change of the ratio between the TP and PP diads with decreasing PP diads and increasing TP diads, an indication of the randomization process (Fig. 3b). During this third phase of the reaction (after ca. 10 h for the reaction at 130 °C), both monomers had been consumed and only transesterification was detected, reaching full randomization after ca. 26 h at 130 °C. Complete randomization was reached when the TP:PP ratio reaches the monomer feed ratio TMC: EtPPn. During the transesterification process, the polymerized EtPPn units can also be transformed into terminal units of a copolymer chain. From our previous studies, we know that PPEs depolymerize by a backbiting mechanism, which releases cyclic PE monomers.[31] The cyclic PE structures exhibit a significant downfield shift in ^{31}P NMR, similar to the EtPPn monomer at ca. 51 ppm compared to the polymeric signals at ca. 34 ppm. When we analyzed the copolymerization and subsequent transesterification, also in the later stages of the reaction, a small signal close to the monomer's resonance was detected in the ^{31}P NMR spectra. This signal can be explained by the fact that during the transesterification, EtPPn units can become terminal units, which allows the formation of a cyclic monomer species in small amounts (ca. 5 %, which is in the range of the equilibrium concentration of phospholanes).[32] The randomization was also achieved by heating a previously prepared gradient polymer **3a** at 130 °C, which resulted in a random copolymer (Fig. S11). All copolymers exhibited a single glass transition temperature between −24 and −29 °C (cf. Table 1), i.e. lower than the T_g of PTMC with ca. −19 °C.[20] The lower glass transition temperatures are expected as the homopolymer of PEtPPn exhibits a T_g of ca. −45 °C, similar to other PPEs prepared by ROP of dioxaphospholanes.[25].

3. Conclusions

We synthesized the first P(EtPPn-*co*-TMC) copolymers in solution and the bulk by statistical copolymerization of trimethylene carbonate and 2-ethyl-2-oxo-1,3,2-dioxaphospholane. Depending on the chosen reaction conditions, different reactivity ratios and thus different gradient copolymers were obtained with the phosphorus-containing monomer being the faster monomer under these conditions. The copolymerizations were monitored in alternating real-time NMR measuring ^{1}H and ^{31}P spectra and reactivity ratios were calculated. After consumption of both monomers, the obtained gradient copolymers were randomized by transesterification in the presence of $Sn(Oct)_2$ at 130 °C. The phosphorus-containing EtPPn monomer is an ideal probe in *real-time* NMR measurements to determine the copolymer microstructure. The sharp signals in the ^{31}P NMR spectra allowed for studying the formation of different diads and triads in during the copolymerization and the calculation of reactivity ratios. The change of diads/ triads after full monomer consumption was used to monitor the transesterification and thus the randomization of the copolymers. This detailed information about the polymer microstructure and the kinetics of the copolymerization gives the possibility to fine-tune the properties of copolymers. The concept of using a P-comonomer as a probe could be transferred to other copolymers, to monitor reaction kinetics and microstructure formation. With the chemical versatility of PPEs, an ideal toolbox to introduce functional groups in diverse copolymer structures, obtained by ring-opening polymerization of cyclic esters and carbonates, is possible, which will be reported by our groups in due course.

4. Experimental

4.1. Materials and methods

4.1.1. Materials

All solvents were purchased in HPLC grade or dry (purity > 99.8 %) and chemicals were purchased in the highest grade (purity > 98 %) from *Sigma Aldrich, Acros Organics, Fluka* or *Fisher Scientific* and used as received unless otherwise described. 1,8-Diazabicyclo[5.4.0]undec-7-ene (DBU) was distilled from calcium hydride and stored over molecular sieves (3 and 4 Å) under a nitrogen atmosphere. 2-(Benzyloxy) ethanol was purchased from *ABCR*, distilled from calcium hydride, and stored over molecular sieves (4 Å) under a nitrogen atmosphere. Ethylene glycol was purchased dry and stored over molecular sieves (4 Å) under nitrogen atmosphere. 2-ethly-2-oxo-1,3,2-dioxaphospholane (EtPPn) was synthesised according to two-step procedure described by Wolf *et al.* [25] The monomer was stored at −25 °C under a nitrogen atmosphere and was freshly distilled before use. Trimethylene carbonate (TMC) was provided by Huizhou Foryou Medical Devices Co., ltd. (China) and used as received.

4.1.1.1. Nuclear Magnetic Resonance (NMR) spectroscopy. ^{1}H, ^{13}C and ^{31}P NMR spectra were measured on a 400 MHz *Bruker AVANCE III AMX system* or 600 MHz *Bruker AVANCE NEO system.* The temperature was kept at 25 °C during the measurements. As deuterated solvents $CDCl_3$ were used. *MestReNova 9* from *Mestrelab Research S.L.* was used for analysis of all measured spectra. The spectra were calibrated against the solvent signal ($CDCl_3$: δH = 7.26 ppm).

For real-time ^{1}H NMR measurements in CH_2Cl_2 a D1 time of 10 *sec* (8 scans) was used and for ^{31}P NMR measurements a D1 time of 30 *sec* (8 scans). For real-time ^{1}H NMR measurements in bulk a D1 time of 15 or 20 *sec* (4 scans) (T1 for all components were determined < 6 *sec*) was used and for ^{31}P NMR measurements a D1 time of 30 or 36 *sec* (4 scans) (T1 for the EtPPn monomer 7.1 *sec* and in the polymer 2.3 *sec*).

4.1.1.2. Gel Permeation Chromatography (GPC). GPC measurements were performed in DMF at 50 °C with an *Agilent Technologies 1260 Infinity PSS SECcurity system* at a flow rate of 1 mL min^{-1}. Each sample injection volume was 50 μL, SDV columns (PSS) with dimensions of 300 × 80 mm^2, 10 μm particle size and pore sizes of 10^6, 10^4, and 500 Å were employed. Calibration was carried out using polystyrene standards supplied by *Polymer Standards Service*. The GPC data were plotted using the software *OriginPro 8G* from *OriginLab Corporation*.

4.1.1.3. Differential Scanning Calorimetry (DSC). DSC measurements were performed using a Trios DSC 25 series thermal analysis system the temperature range from −100 °C to 35 °C under nitrogen with a heating rate of 10 °C min-1. All glass transition temperatures (T_g) were obtained from the second heating ramp of the experiment.

4.1.2. Syntheses

4.1.2.1. Copolymerization of EtPPn and TMC in solution. In a flame-dried Schlenk tube, TMC (730 mg, 7.15 mmol, 4350 eq) and EtPPn (139 mg, 1.02 mmol, 600 eq) were dissolved in anhydrous benzene (6 mL) and dried by lyophilization. The monomer mixture was dissolved in anhydrous dichloromethane (2 mL, 4 M) and the calculated amount of a stock solution (0.2 mol/L) of 2-(benzyloxy)ethanol in dry dichloromethane (15 μL, 1 eq) was added. 0.7 mL of this solution were transferred with a syringe in a dry NMR tube and closed with a septum. All measuring parameters were determined on the pre reaction mixture. The reaction was initiated by the addition of 150 μL (50 eq) of an DBU stock solution (0.2 mol/L in DCM). The tube was placed in the NMR spectrometer (at 25 °C) and ^{1}H and ^{31}P NMR measurements were run alternating. The copolymerization was terminated after 45 h by the rapid addition of 0.5

mL formic acid dissolved in dichloromethane (20 mg mL^{-1}). Purification was performed by precipitation into cold diethyl ether (ca. −5 °C, 40 mL) and the polymer was recovered after centrifugation (4000 rpm, 10 min, 5 °C). The material was dissolved again in ca. 5 mL dichloromethane and the precipitation procedure repeated. Then, the polymer was dried in a *vacuo* over night to obtain a colourless sticky material. (when the polymerization is conducted in a flask typical yields are ca. 90 %).

4.1.2.2. Copolymerization of EtPPn and TMC in the bulk. In a flame-dried Schlenk tube, TMC (1.82 g, 17.8 mmol), EtPPn (226 mg, 1.7 mmol) and $Sn(Oct)_2$ (10.1 mg, 0.02 mmol) were dissolved in anhydrous benzene (8 mL) and dried by lyophilization two times, the second time over night. The monomer mixture was heated to 70 °C and 0.7 mL were transferred into a dry NMR tube. After cooling the mixture to room temperature, the NMR tube was evacuated (ca. $2*10^{-3}$ mbar) and flame-sealed. The closed NMR tube was stored at −25 °C until the NMR measurement were performed. After, the tube was placed in the pre heated NMR machine at the respective temperature (120 or 130 °C) and all measuring parameters were determined. ^{1}H and ^{31}P NMR measurements were run alternating. The reaction was stopped by cooling to room temperature. The polymer was collected after the ampule was opened, the crude was dissolved in ca. 20 mL DCM and precipitated into cold diethyl ether (ca. −5 °C, 200 mL). The material was dissolved again in ca. 10 mL dichloromethane and the precipitation procedure repeated. Then, the polymer was dried in *vacuo* over night to obtain the pure copolymer as a colourless sticky material (when the polymerization is conducted in a flask typical yields are ca. 90 %).

CRediT authorship contribution statement. **Timo Rheinberger:** Data curation, Formal analysis, Investigation, Writing – original draft, Writing – review & editing, Methodology. **Marc Ankone:** Investigation, Methodology, Validation. **Dirk Grijpma:** Conceptualization, Funding acquisition, Supervision. **Frederik R. Wurm:** Conceptualization, Formal analysis, Funding acquisition, Supervision, Writing – original draft, Writing – review & editing.

Declaration of Competing Interest

The authors declare that they have no known competing financial interests or personal relationships that could have appeared to influence the work reported in this paper.

Data availability

Data will be made available on request.

Acknowledgements

We are thankful for the technical support from Bianca H.M. Ruel (Univ. Twente) for NMR measurements.

Data availability

Data will be made available upon request.

Appendix A. Supplementary material

Supplementary data to this article can be found online at https://doi.org/10.1016/j.eurpolymj.2022.111607.

References

[1] R. Shi, D. Chen, Q. Liu, Y. Wu, X. Xu, L. Zhang, W. Tian, Recent advances in synthetic bioelastomers, Int. J. Mol. Sci. 10 (10) (2009) 4223–4256.
[2] M.F. Maitz, Applications of synthetic polymers in clinical medicine, Biosurf. Biotribol. 1 (3) (2015) 161–176.
[3] T. Haider, C. Völker, J. Kramm, K. Landfester, F.R. Wurm, Plastics of the future? The impact of biodegradable polymers on the environment and on society, Angew. Chem. Int. Ed. (2018), https://doi.org/10.1002/anie.201805766.
[4] Q. Song, C. Pascouau, J. Zhao, G. Zhang, F. Peruch, S. Carlotti, Ring-opening polymerization of γ-lactones and copolymerization with other cyclic monomers, Prog. Polym. Sci. 110 (2020), 101309.
[5] B.F. Lee, M. Wolffs, K.T. Delaney, J.K. Sprafke, F.A. Leibfarth, C.J. Hawker, N. A. Lynd, Reactivity ratios and mechanistic insight for anionic ring-opening copolymerization of epoxides, Macromolecules 45 (9) (2012) 3722–3731.
[6] G. Becker, F.R. Wurm, Functional biodegradable polymers via ring-opening polymerization of monomers without protective groups, Chem. Soc. Rev. 47 (20) (2018) 7739–7782.
[7] G. Rokicki, Aliphatic cyclic carbonates and spiroorthocarbonates as monomers, Prog. Polym. Sci. 25 (2) (2000) 259–342.
[8] L. Mespouille, O. Coulembier, M. Kawalec, A.P. Dove, P. Dubois, Implementation of metal-free ring-opening polymerization in the preparation of aliphatic polycarbonate materials, Prog. Polym. Sci. 39 (6) (2014) 1144–1164.
[9] K. Fukushima, Poly(trimethylene carbonate)-based polymers engineered for biodegradable functional biomaterials, Biomater. Sci. 4 (1) (2016) 9–24.
[10] K.N. Bauer, H.T. Tee, M.M. Velencoso, F.R. Wurm, Main-chain poly(phosphoester) s: History, syntheses, degradation, bio-and flame-retardant applications, Prog. Polym. Sci. 73 (2017) 61–122.
[11] T. Steinbach, E.M. Alexandrino, F.R. Wurm, Unsaturated poly(phosphoester)s via ring-opening metathesis polymerization, Polym. Chem. 4 (2013) 3800–3806.
[12] T. Steinbach, R. Schroder, S. Ritz, F.R. Wurm, Microstructure analysis of biocompatible phosphoester copolymers, Polym. Chem. 4 (16) (2013) 4469–4479.
[13] T. Pakula, K. Matyjaszewski, Copolymers with controlled distribution of comonomers along the chain, 1. Structure, thermodynamics and dynamic properties of gradient copolymers. Computer simulation, Macromol. Theory Simul. 5 (5) (1996) 987–1006.
[14] Y. Shapiro, Analysis of chain microstructure by 1H and 13C NMR spectroscopy, Bulletin of Magnetic, Resonance 7 (1985) 27–58.
[15] J. Kasperczyk, Microstructural analysis of poly[(l, l-lactide)-co-(glycolide)] by 1H and 13C n.m.r. spectroscopy, Polymer 37 (2) (1996) 201–203.
[16] A. Natalello, A. Alkan, P. Von Tiedemann, F.R. Wurm, H. Frey, Functional group distribution and gradient structure resulting from the living anionic copolymerization of styrene and para-But-3-enyl styrene, ACS Macro Lett. 3 (6) (2014) 560–564.
[17] E. Rieger, A. Alkan, A. Manhart, M. Wagner, F.R. Wurm, Sequence-Controlled polymers via simultaneous living anionic copolymerization of competing monomers, Macromol. Rapid Commun. 37 (10) (2016) 833–839.
[18] A. Alkan, A. Natalello, M. Wagner, H. Frey, F.R. Wurm, Ferrocene-containing multifunctional polyethers: monomer sequence monitoring via quantitative 13C NMR spectroscopy in bulk, Macromolecules 47 (7) (2014) 2242–2249.
[19] G. Becker, Z. Deng, M. Zober, M. Wagner, K. Lienkamp, F.R. Wurm, Surface-attached poly (phosphoester)-hydrogels with benzophenone groups, Polym. Chem. 9 (3) (2018) 315–326.
[20] A.P. Pêgo, D.W. Grijpma, J. Feijen, Enhanced mechanical properties of 1,3-trimethylene carbonate polymers and networks, Polymer 44 (21) (2003) 6495–6504.
[21] L. Yang, J. Li, W. Zhang, Y. Jin, J. Zhang, Y. Liu, D. Yi, M. Li, J. Guo, Z. Gu, The degradation of poly(trimethylene carbonate) implants: The role of molecular weight and enzymes, Polym. Degrad. Stab. 122 (2015) 77–87.
[22] H. Goldmann, H. Hierlemann, E. Mueller, H. Planck, Surgical suture material and method of making and using same, Google Patents (1997).
[23] H.R. Kricheldorf, I. Kreiser-Saunders, C. Boettcher, Polylactones, 31. Sn(II)octoate-initiated polymerization of L-lactide: a mechanistic study, Polymer 36 (6) (1995) 1253–1259.
[24] A. Casas, M.J. Ramos, J.F. Rodríguez, Á. Pérez, Tin compounds as Lewis acid catalysts for esterification and transesterification of acid vegetable oils, Fuel Process. Technol. 106 (2013) 321–325.
[25] T. Wolf, T. Steinbach, F.R. Wurm, A Library of Well-Defined and Water-Soluble Poly(alkyl phosphonate)s with Adjustable Hydrolysis, Macromolecules 48 (12) (2015) 3853–3863.
[26] F. Nederberg, B.G.G. Lohmeijer, F. Leibfarth, R.C. Pratt, J. Choi, A.P. Dove, R. M. Waymouth, J.L. Hedrick, Organocatalytic ring opening polymerization of trimethylene carbonate, Biomacromolecules 8 (1) (2007) 153–160.
[27] V. Jaacks, A novel method of determination of reactivity ratios in binary and ternary copolymerizations, Die Makromolekulare Chemie: Macromolecular Chemistry and Physics 161 (1) (1972) 161–172.
[28] B.S. Beckingham, G.E. Sanoja, N.A. Lynd, Simple and accurate determination of reactivity ratios using a nonterminal model of chain copolymerization, Macromolecules 48 (19) (2015) 6922–6930.
[29] J. Blankenburg, E. Kersten, K. Maciol, M. Wagner, S. Zarbakhsh, H. Frey, The poly (propylene oxide-co-ethylene oxide) gradient is controlled by the polymerization method: determination of reactivity ratios by direct comparison of different copolymerization models, Polym. Chem. 10 (22) (2019) 2863–2871.
[30] T. Gleede, J.C. Markwart, N. Huber, E. Rieger, F.R. Wurm, Competitive copolymerization: access to aziridine copolymers with adjustable gradient strengths, Macromolecules 52 (24) (2019) 9703–9714.
[31] K.N. Bauer, L. Liu, M. Wagner, D. Andrienko, F.R. Wurm, Mechanistic study on the hydrolytic degradation of polyphosphates, Eur. Polym. J. 108 (2018) 286–294.
[32] C.-S. Xiao, Y.-C. Wang, J.-Z. Du, X.-S. Chen, J. Wang, Kinetics and mechanism of 2-Ethoxy-2-oxo-1,3,2-dioxaphospholane polymerization initiated by stannous octoate, Macromolecules 39 (20) (2006) 6825–6831.